Available online at www.sciencedirect.com

ScienceDirect

Nuclear Physics B 923 (2017) 588–607

NUCLEAR PHYSICS B

www.elsevier.com/locate/nuclphysb

Matrix pentagons

A.V. Belitsky

Department of Physics, Arizona State University, Tempe, AZ 85287-1504, USA

Received 21 May 2017; received in revised form 18 July 2017; accepted 15 August 2017
Available online 31 August 2017
Editor: Stephan Stieberger

Abstract

The Operator Product Expansion for null polygonal Wilson loop in planar maximally supersymmetric Yang–Mills theory runs systematically in terms of multi-particle pentagon transitions which encode the physics of excitations propagating on the color flux tube ending on the sides of the four-dimensional contour. Their dynamics was unraveled in the past several years and culminated in a complete description of pentagons as an exact function of the 't Hooft coupling. In this paper we provide a solution for the last building block in this program, the SU(4) matrix structure arising from internal symmetry indices of scalars and fermions. This is achieved by a recursive solution of the Mirror and Watson equations obeyed by the so-called singlet pentagons and fixing the form of the twisted component in their tensor decomposition. The non-singlet, or charged, pentagons are deduced from these by a limiting procedure.

1. Introduction

A framework for a systematic analysis of the multi-collinear limit of the super Wilson loop in planar $\mathcal{N} = 4$ super Yang–Mills theory on a four-dimensional null polygonal contour was proposed in Refs. [1,2]. It is akin to the Operator Product Expansion for correlation functions of local operators. The limit of adjacent segments of the loop as they approach the same null line introduces curvature field insertions into the Wilson link stretched along this direction. These in turn correspond to excitations on top of the Faraday flux tube. Their integrable dynamics was

E-mail address: andrei.belitsky@asu.edu.

http://dx.doi.org/10.1016/j.nuclphysb.2017.08.011

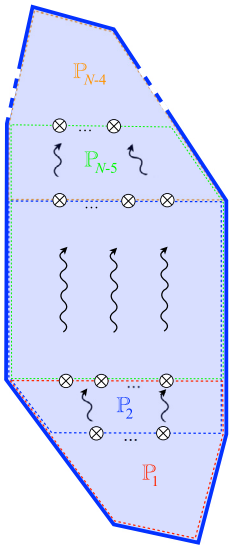

Fig. 1. A tessellation of the polygon into pentagons with a sample set of insertions of flux-tube excitations from the resolution of the identity operator on the inner null lines (shown by the $\otimes$ symbols). These propagate from the bottom to the top and interact with each other along the way.

scrutinized in the context of the large-spin limit of high-twist single-trace Wilson operators in the maximally supersymmetric Yang–Mills theory [3] and is known at any value of the 't Hooft coupling [4].

A geometric tessellation of the N-gon superloop $\mathbb{W}_N$ in null squares introduces the main building block of the formalism, the pentagon $\mathbb{P}$, formed by two adjacent squares, yielding the representation

$$\mathbb{W}_N = \langle 0|\mathbb{P}_{N-4}\dots\mathbb{P}_2\mathbb{P}_1|0\rangle\,. \tag{1.1}$$

The resolution of the unit operators between sequential pentagons produces the decomposition of the superloop in terms of transition matrix elements of multi-particle flux-tube excitations $|\mathbf{p}_N\rangle \equiv |\mathrm{p}_1\mathrm{p}_2\dots\mathrm{p}_N\rangle$ propagating with respective rapidities $\boldsymbol{u} = (u_1, u_2, \dots, u_N)$ and interacting on the two-dimensional world-sheet of the loop (see Fig. 1 for a graphical representation),

$$\mathbb{W}_N = \sum\!\!\!\!\!\!\int_{N,N',\dots,N''} \langle 0|\mathbb{P}_{N-4}|\mathbf{p}_{N''}(\boldsymbol{u}'')\rangle\dots\langle\mathbf{p}_{N'}(\boldsymbol{u}')|\mathbb{P}_2|\mathbf{p}_N(\boldsymbol{u})\rangle\langle\mathbf{p}_N(\boldsymbol{u})|\mathbb{P}_1|0\rangle\,, \tag{1.2}$$

where we did not display for brevity the $N-5$ accompanying propagation phases or integration measures. The subscripts on the flux-tube excitations cumulatively stand for their Lorentz spins and internal symmetry indices. The single-particle spectrum consists of (anti)gluons, scalars, aka holes,[1] and (anti)fermions $|\mathrm{p}\rangle = |\bar{\mathrm{g}}\rangle, |\mathrm{g}\rangle, |\mathrm{h}^{AB}\rangle, |\bar{\Psi}_A\rangle, |\Psi^A\rangle$, which transform in the $\mathbf{1}, \mathbf{1}, \mathbf{6}, \bar{\mathbf{4}}, \mathbf{4}$ of the SU(4) internal symmetry group. In the above formula, the pentagon (or rather the su-

[1] One can pass to O(6) indices instead making use of the 4×4 off-diagonal blocks $\Sigma_{I,AB}$ of the six-dimensional Dirac matrices in Euclidean metric, such that $\mathrm{h}^{AB} = \Sigma^{I,AB}\mathrm{h}^I/\sqrt{2}$. These obey the following involution properties $(\Sigma^{I,AB})^* = \overline{\Sigma}^I_{AB} \equiv \varepsilon_{ABCD}\Sigma^{I,CD}/2$.

perpentagon) $\mathbb{P}$ admits a terminating series in increasing powers of the Grassmann variable θ_A, carrying the index of the antifundamental representation of SU(4),

$$\mathbb{P} = \mathcal{P} + \theta_A \mathcal{P}^A + \tfrac{1}{2!}\theta_A\theta_B \mathcal{P}^{AB} + \tfrac{1}{3!}\theta_A\theta_B\theta_C \mathcal{P}^{ABC} + \tfrac{1}{4!}\theta_A\theta_B\theta_C\theta_D \mathcal{P}^{ABCD}\,, \tag{1.3}$$

starting with the singlet $\mathcal{P}$ followed by the SU(4) non-singlet, or charged, operators $\mathcal{P}^A$, $\mathcal{P}^{AB}$ etc.

The matrix elements in (1.2) can be written in the form

$$\langle \mathbf{p}_{N'}(\boldsymbol{v})|\mathcal{P}^{A\cdots}|\mathbf{p}_N(\boldsymbol{u})\rangle = [\Pi^{A\cdots}]_{N|N'}(\boldsymbol{u}|\boldsymbol{v})\, P(\boldsymbol{u}|\boldsymbol{v})\,, \tag{1.4}$$

where the second factor $P(\boldsymbol{u}|\boldsymbol{v})$ depends on the dynamics of the flux-tube excitations and was the subject of intensive research over the past several years [5–12]. In fact, it possesses a factorized form in terms of one-to-one particle pentagon transitions [5,10] as was rigorously demonstrated at leading order in 't Hooft coupling g in the context of open (super)spin chains for the flux tube [13,14]. While the first (matrix) factor $\Pi^{A\cdots}_{N|N'}(\boldsymbol{u}|\boldsymbol{v})$ encodes information on the internal symmetry indices and enjoys rational dependence on differences of particles' rapidities. It is independent of g and is thus purely kinematical in origin. It is the focus of the present work. At this point, it is worth pointing out that both of the above facts are, in principle, conjectures. However, they withstood all tests conducted to date against explicit data on scattering amplitudes made available by other means and methods. For the case at hand, the uniqueness of matrix part was again verified purely empirically as will be further discussed later.

Our subsequent presentation is organized as follows. In the next section, we start with the matrix elements of the singlet pentagon operator involving only holes and provide a systematics procedure for construction of all terms in its tensor decomposition which is based on the solution of Mirror and Watson equations obeyed by matrix pentagons. The seed for this recursion is provided by just one component which requires absolute fixing. Next, we move on to the purely fermion helicity-preserving transitions. Then we conclude with mixed fermion–hole singlet pentagons and finally with the transition involving all charged excitations. In Sect. 3, we address the question of moving excitations from the initial to final state, giving an effective set of rules for fermions which lack a simple one-particle mirror transformation. We then demonstrate how to deduce the non-singlet transitions in Sect. 4 from the ones we just computed. We construct integrands of polygon loops in the flux-tube representation and verify our findings by comparing them with the integral representation suggested in Refs. [15,16] for the hexagonal Wilson loop in Sect. 5, finding agreement. In Appendix A we give a few examples of tensors with small number of particles, leaving the rest to the accompanying Mathematica notebook that contains routines for automatic solution of systems of Mirror and Watson equations, testing results against integral representation of the hexagon and limiting procedure to obtain all transition matrices from the minimal set considered in this paper.

2. Singlet pentagons

To begin with, we address the matrix structure of the lowest Grassmann component $\mathcal{P}$ in the expansion of the superpentagon $\mathbb{P}$. We will discuss in turn three cases of increasing complexity from purely hole transition matrix elements passing to purely fermionic ones and finally addressing their mixed states.

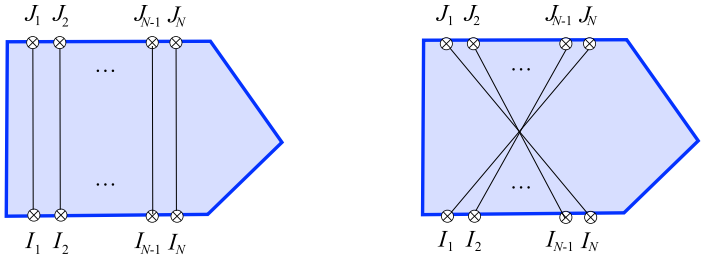

Fig. 2. Two contributions out of $(2N-1)!!$ of perfect pairings of O(6) indices of holes which are displayed in Eq. (2.4). The picture on the right shows the twisted graph which corresponds to the seed rational function for the recursive solution of the defining equations.

2.1. Hole matrices

We start with a comment. The singlet pentagon operator itself obviously does not carry any SU(4) indices, so its matrix elements can have a total even number of holes shared between the initial and final states. In this section we provide a solution to the diagonal N-to-N case. The particle number-changing transitions can be deduced from this one making use of the known double Wick, aka mirror, transformation properties which allow one to move excitations between different sides of the pentagon.

With this in mind, let us introduce transitions from the initial state of N scalars carrying rapidities $\boldsymbol{u} = (u_1, \dots, u_N)$ and O(6) indices[2] $\boldsymbol{I} = (I_1, \dots, I_N)$, cumulatively called $\mathbf{h}^{\boldsymbol{I}}(\boldsymbol{u})$, to the final state of N scalars $\mathbf{h}^{\boldsymbol{J}}(\boldsymbol{v})$,

$$P^{\boldsymbol{I}|\boldsymbol{J}}(\boldsymbol{u}|\boldsymbol{v}) = \langle \mathbf{h}^{\boldsymbol{J}}(\boldsymbol{v})|\mathcal{P}|\mathbf{h}^{\boldsymbol{I}}(\boldsymbol{u})\rangle\,. \tag{2.1}$$

The above pentagons can be cast in the form of a scalar factor accompanied by an O(6) tensor

$$P^{\boldsymbol{I}|\boldsymbol{J}}(\boldsymbol{u}|\boldsymbol{v}) = \Pi^{\boldsymbol{I}|\boldsymbol{J}}(\boldsymbol{u}|\boldsymbol{v})\,P_{\mathbf{h}|\mathbf{h}}(\boldsymbol{u}|\boldsymbol{v})\,. \tag{2.2}$$

Here $P_{\mathbf{h}|\mathbf{h}}(\boldsymbol{u}|\boldsymbol{v})$ contains dynamical information about the transition of N-to-N hole states through the dependence on the 't Hooft coupling. It was shown to admit a factorized form in terms of two-particle pentagons [5,10,13,14]

$$P_{\mathbf{h}|\mathbf{h}}(\boldsymbol{u}|\boldsymbol{v}) = \frac{\prod\limits_{i,j}^{N} P_{\mathrm{h}|\mathrm{h}}(u_i|v_j)}{\prod\limits_{i>j}^{N} P_{\mathrm{h}|\mathrm{h}}(u_i|u_j)\prod\limits_{i<j}^{N} P_{\mathrm{h}|\mathrm{h}}(v_i|v_j)}\,. \tag{2.3}$$

As was already stated in the Introduction, the matrix $\Pi^{\boldsymbol{I}|\boldsymbol{J}}(\boldsymbol{u}|\boldsymbol{v})$ does not depend on the coupling constant and, as a function of the rapidity variables, it enjoys dependence only through their differences and is purely rational in nature. Its tensor decomposition runs over $(2N-1)!!$ perfect pairings of all indices[3]

[2] We will find useful using the SU(4) indices instead when discussing mixed matrix elements. For the time being the O(6) conventions are the most economical.

[3] We adopt the numbering scheme that naturally emerges from a pairing routine in the accompanying Mathematica notebook.

$$\Pi^{\boldsymbol{I}|\boldsymbol{J}}(\boldsymbol{u}|\boldsymbol{v}) = \ldots + \delta^{I_1 J_1}\delta^{I_2 J_2}\delta^{I_3 J_3}\ldots\delta^{I_N J_N}\pi_{[(2N-1)!!+1]/2}(\boldsymbol{u}|\boldsymbol{v}) + \ldots + \delta^{I_1 J_N}\delta^{I_2 J_{N-1}}\delta^{I_3 J_{N-2}}\ldots\delta^{I_N J_1}\pi_{(2N-1)!!}(\boldsymbol{u}|\boldsymbol{v})\,, \tag{2.4}$$

shown schematically in Fig. 2. The last matrix structure corresponds to the twisted graph, i.e., when the ordering on all of the sites on the top is completely reversed, i.e., $(123\ldots N) \to (N\ldots 321)$. It will play a distinguished role in our consideration. In principle, one could introduce extra tensor structures involving odd number of SO(6) Levi-Civita symbols for each sextet of holes. However, solution to Mirror and Watson equation combined with Bose symmetry do not yield nontrivial solutions for the corresponding structures. Thus, they will be ignored in what follows.

2.1.1. Solution to Mirror and Watson equations

The matrix pentagon (2.2) obeys a system of defining relations. It is formed by the Mirror and Watson equations. The first of this kind emerges from the invariance of the flux-tube background with respect to the double Wick rotation [1], which allows one to interchange space and time variables on the two-dimensional worldsheet of the loop. From the point of view of the hole excitation, this interchanges the energy and momentum in its dispersion relation. As a function of the rapidity variable, an analytic continuation that accomplishes this goal was found in Ref. [17]. For the hole-to-hole pentagon transition, it takes the following form [5]

$$P_{\mathrm{h}|\mathrm{h}}(u|v^{\gamma}) = P_{\mathrm{h}|\mathrm{h}}(v|u)\,, \tag{2.5}$$

where γ stands for the aforementioned path in the complex rapidity plane. In fact, since $P_{\mathrm{h}|\mathrm{h}}(u|v)$ is a meromorphic function of rapidities with an infinite number of cuts equidistantly spaced along the imaginary axis $[-2g + i(k+\frac{1}{2}), 2g + i(k+\frac{1}{2})]$, with $k \in \mathbb{Z}$, the continuation $v^{\gamma} = v + i$ implies going through the lowest cut in the upper half-plane and passing to another (mirror) Riemann sheet [17,18]. Multiple application of the mirror transformation to the same excitation allows one to move it from the initial to the final state, yielding a creation form factor [5]

$$P_{\mathrm{h}|\mathrm{h}}(u^{2\gamma}|v) = \frac{R_{\mathrm{hh}}(u,v)}{P_{\mathrm{h}|\mathrm{h}}(u|v)}\,, \qquad R_{\mathrm{hh}}(u,v) = \frac{1}{(u|v)_1(u|v)_2}\,. \tag{2.6}$$

It is related to the inverse of the original transition pentagon up to an overall rational function $R_{\mathrm{hh}}(u,v)$ of hole rapidities. Here and below, we use the notation

$$(u|v)_{\sigma} \equiv u - v + i\sigma \tag{2.7}$$

to make expressions more compact. Obviously, $(u|v)_{\sigma} = -(v|u)_{-\sigma}$.

For the multi-hole matrix pentagon (2.1), moving α excitations from the top to bottom and the same number of the bottom ones to the top, say, in the clockwise direction, yields the same object but with accordingly changed rapidities and O(6) matrix structure. The Mirror equations, shown diagrammatically by the top panel in Fig. 3, then read

$$P^{\boldsymbol{I}|\boldsymbol{J}}(\boldsymbol{u} + 2i\boldsymbol{\alpha}|\boldsymbol{v} + 3i\bar{\boldsymbol{\alpha}}) = P^{I_{\alpha+1},\ldots,I_N,J_N,\ldots,J_{N-\alpha+1}|I_{\alpha},\ldots,I_1,J_1,\ldots,J_{N-\alpha}}(u_{\alpha+1},\ldots,u_N,v_N,\ldots,v_{N-\alpha+1}| u_{\alpha},\ldots,u_1,v_1,\ldots,v_{N-\alpha})\,. \tag{2.8}$$

Here we introduced vectors $\boldsymbol{\alpha}$ and $\bar{\boldsymbol{\alpha}}$ with unit components

$$\boldsymbol{\alpha} = (\overbrace{1,\ldots,1}^{\alpha},0,\ldots 0)\,, \qquad \bar{\boldsymbol{\alpha}} = (0,\ldots,0,\overbrace{1,\ldots,1}^{\alpha}) \tag{2.9}$$

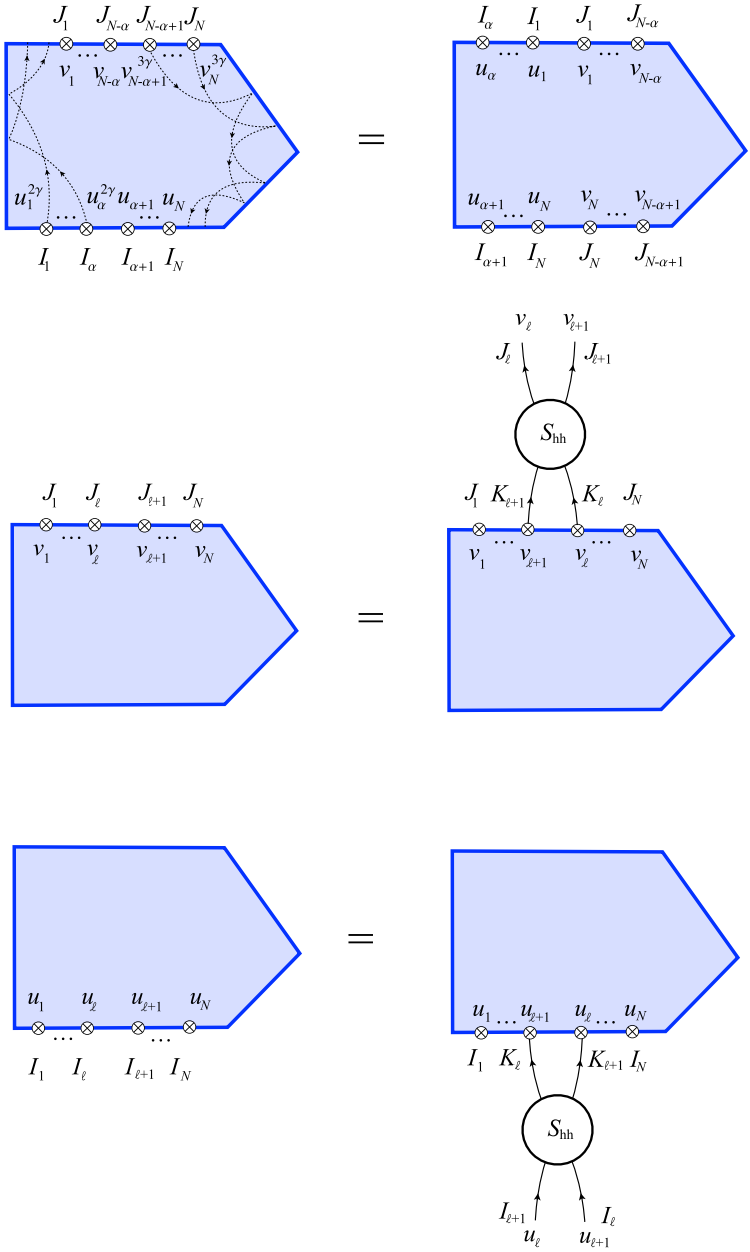

Fig. 3. From top to bottom: Graphical representation of the Mirror and Watson equations for (top and bottom) hole flux-tube excitations.

and their length $\alpha = |\boldsymbol{\alpha}| = |\bar{\boldsymbol{\alpha}}|$.

The Watson equations can be written either for the initial or final state. They are, respectively,

$$P^{\boldsymbol{I}|\boldsymbol{J}}(\boldsymbol{u}|\boldsymbol{v}) = S^{I_{\ell+1}I_\ell|K_{\ell+1}K_\ell}(u_\ell, u_{\ell+1})\, P^{I_1,\ldots,K_{\ell+1},K_\ell,\ldots,I_N|\boldsymbol{J}}(u_1,\ldots,u_{\ell+1},u_\ell,\ldots,u_N|\boldsymbol{v})\,, \tag{2.10}$$

$$P^{\boldsymbol{I}|\boldsymbol{J}}(\boldsymbol{u}|\boldsymbol{v}) = S^{K_{\ell+1}K_\ell|J_{\ell+1}J_\ell}(v_{\ell+1}, v_\ell)\, P^{\boldsymbol{I}|J_1,\ldots,K_{\ell+1},K_\ell,\ldots,J_N}(\boldsymbol{u}|v_1,\ldots,v_{\ell+1},v_\ell,\ldots,v_N)\,, \tag{2.11}$$

with $1 \le \ell \le N-1$ and where the S-matrix for scattering of the sextet of scalar excitations

$$\begin{aligned} &S^{I_1I_2|J_1J_2}(u,v) \\ &= S_{\rm hh}(u,v)\left[\delta^{I_1J_1}\delta^{I_2J_2}s^{(1)}_{\rm hh}(u,v) + \delta^{I_1J_2}\delta^{I_2J_1}s^{(2)}_{\rm hh}(u,v) + \delta^{I_1I_2}\delta^{J_1J_2}s^{(3)}_{\rm hh}(u,v)\right], \end{aligned} \tag{2.12}$$

differs from the Zamolodchikovs' O(6) matrix by the overall dynamical phase $S_{\rm hh}(u,v)$ that encodes information on the flux-tube background as a function of the 't Hooft coupling. The nested Bethe Ansatz uniquely determines the rational factors in front of the identity, permutation and annihilation tensors [19]

$$\begin{aligned} &s^{(1)}_{\rm hh}(u,v) = \frac{u-v}{u-v-i}\,, \qquad s^{(2)}_{\rm hh}(u,v) = \frac{-i}{u-v-i}\,, \\ &s^{(3)}_{\rm hh}(u,v) = \frac{i(u-v)}{(u-v-i)(u-v-2i)}\,, \end{aligned} \tag{2.13}$$

respectively. The two equations, (2.10) and (2.11), contain identical information, so only one of them provides an independent set of relations between π-functions. As a consequence, one is free to choose one of the above for the recursive solution of form factors in question.

It is important to realize that the Watson equation alone is not sufficient in general to determine all coefficients recursively. One has to rely on the Mirror equation as well to express all π's in terms of just one, $\pi_{(2N-1)!!}(\boldsymbol{u}|\boldsymbol{v})$, in front of the twisted matrix structure. This last one has to be absolutely fixed and the most stringent constraint for it arises from the Mirror equations. The latter are specific to the flux-tube dynamics of the maximally supersymmetric Yang–Mills theory and, therefore, cannot be used in a generic form factor program. They read

$$\begin{aligned} &\frac{\pi_{(2N-1)!!}(u_{\alpha+1},\ldots,u_N,v_N,\ldots,v_{N-\alpha+1}|u_\alpha,\ldots,u_1,v_1,\ldots,v_{N-\alpha})}{\pi_{(2N-1)!!}(\boldsymbol{u}+2i\boldsymbol{\alpha}|\boldsymbol{v}+3i\bar{\boldsymbol{\alpha}})} \\ &= \frac{\prod\limits_{j_1=1}^{\alpha}\prod\limits_{k_1=\alpha+1}^{N}(u_{j_1}|u_{k_1})_0(u_{j_1}|u_{k_1})_1 \prod\limits_{j_2=N-\alpha+1}^{N}\prod\limits_{k_2=1}^{N-\alpha}(v_{k_2}|v_{j_2})_{-1}(v_{k_2}|v_{j_2})_{-2}}{\prod\limits_{j_1=1}^{\alpha}\prod\limits_{k_1=1}^{N-\alpha}(u_{j_1}|v_{k_1})_1(u_{j_1}|v_{k_1})_2 \prod\limits_{j_2=N-\alpha+1}^{N}\prod\limits_{k_2=\alpha+1}^{N}(u_{k_2}|v_{j_2})_{-1}(u_{k_2}|v_{j_2})_{-2}}\,. \end{aligned} \tag{2.14}$$

The origin of the rational function in the right-hand side is traced back to the product of $R_{\rm h|h}$ coefficients in Eq. (2.6). The solution to these equations is given by the quotient of same degree polynomials in rapidity variables in the numerator and denominator,

$$\pi_{(2N-1)!!}(\boldsymbol{u}|\boldsymbol{v}) = \frac{\prod\limits_{k_1=1}^{N-1}\prod\limits_{j_1=1}^{N-k_1}(u_{j_1}|v_{k_1})_0 \prod\limits_{j_2=2}^{N}\prod\limits_{k_2=j_2}^{N-k_2}(u_{j_2}|v_{N-k_2+2})_1}{\prod\limits_{j_1=1}^{N-1}\prod\limits_{k_1=j_1+1}^{N-1}(u_{j_1}|u_{k_1})_{-1}(v_{j_1}|v_{k_1})_1}\,. \tag{2.15}$$

The correctness of this solution was verified by means of dedicated perturbative analyses for low number of particles, see, e.g., Refs. [6,11]. We provide an explicit example for $2 \to 2$ and $3 \to 3$ transitions in Appendix A.1. Expressions for larger number of particles are prohibitively long to be displayed explicitly in the paper and are more suitable in a symbolic form of the accompanying Mathematica notebook.

2.2. Fermion matrices

Let us continue with pentagon transitions involving only fermions, namely, the ones corresponding to N fermions in the initial state and the same number of antifermions in the final state

$$P^{\boldsymbol{A}|}{}_{\boldsymbol{B}}(\boldsymbol{u}|\boldsymbol{v}) = \langle \bar{\boldsymbol{\Psi}}_{\boldsymbol{B}}(\boldsymbol{v})|\mathcal{P}|\boldsymbol{\Psi}^{\boldsymbol{A}}(\boldsymbol{u})\rangle = \Pi^{\boldsymbol{A}|}{}_{\boldsymbol{B}}(\boldsymbol{u}|\boldsymbol{v})P_{\boldsymbol{\Psi}|\boldsymbol{\Psi}}(\boldsymbol{u}|\boldsymbol{v})\,. \tag{2.16}$$

These correspond to the helicity-preserving matrix elements. Notice that the SU(4) symmetry also allows for transitions involving quartets of (anti)fermions in addition to the excitations already present in the in- and out-states due to possibility to carry internal symmetry group indices by the four-dimensional Levi-Civita tensor, however, these will be obtained from the ones we are about to analyze by taking a particular limit.

The decomposition in independent tensors is straightforward and arises from the pairwise contraction of the bottom and top indices with Kronecker symbols and $N!$ permutations of either the top or bottom positions,

$$\Pi^{\boldsymbol{A}|}{}_{\boldsymbol{B}}(\boldsymbol{u}|\boldsymbol{v}) = \delta^{A_1}_{B_1}\delta^{A_2}_{B_2}\ldots\delta^{A_N}_{B_N}\pi_1(\boldsymbol{u}|\boldsymbol{v}) + \cdots + \delta^{A_1}_{B_N}\delta^{A_2}_{B_{N-1}}\ldots\delta^{A_N}_{B_1}\pi_{N!}(\boldsymbol{u}|\boldsymbol{v})\,, \tag{2.17}$$

with displayed terms shown graphically in Fig. 2.

Fermions do not enjoy a simple mirror transformation [6] so we do not have an equation to fix the twisted component. However, by analogy with the case of scalars discussed in the previous section, we anticipate that the rational function should differ from it only marginally, i.e., possibly by the imaginary shifts due to different helicity of the excitations involved if at all. In fact, we conjecture the $\pi_{N!}$ to take the form

$$\pi_{N!}(\boldsymbol{u}|\boldsymbol{v}) = \frac{\prod\limits_{k_1=1}^{N-1}\prod\limits_{j_1=1}^{N-k_1}(u_{j_1}|v_{k_1})_0\prod\limits_{j_2=2}^{N}\prod\limits_{k_2=j_2}^{N-k_2}(u_{j_2}|v_{N-k_2+2})_1}{\prod\limits_{j_1=1}^{N-1}\prod\limits_{k_1=j_1+1}^{N-1}(u_{j_1}|u_{k_1})_{-1}(v_{j_1}|v_{k_1})_1}\,. \tag{2.18}$$

We want to emphasize that this form is intrinsic to the flux-tube dynamics.

This seed provides the solution for the matrix structure in question since all functions accompanying other structures can be extracted making use of the Watson equations alone, contrary to the scalar sector where the number of independent components is much higher and one has to rely on additional relations emerging from the Mirror equations. The Watson equations for the fermion take the same form as Eqs. (2.10)–(2.11) with obvious replacements of O(6) indices on the bottom/top with covariant/contravariant SU(4) indices and the fermion–fermion scattering matrix being

$$S^{A_1A_2}_{B_1B_2}(u,v) = S_{\Psi\Psi}(u,v)\left[\delta^{A_1}_{B_1}\delta^{A_2}_{B_2}s^{(1)}_{\Psi\Psi}(u,v) + \delta^{A_1}_{B_2}\delta^{A_2}_{B_1}s^{(2)}_{\Psi\Psi}(u,v)\right], \tag{2.19}$$

where the component of the R-matrix are [20]

$$s^{(1)}_{\Psi\Psi}(u,v) = \frac{u-v}{u-v-i}\,, \qquad s^{(2)}_{\Psi\Psi}(u,v) = \frac{-i}{u-v-i}\,. \tag{2.20}$$

Due to a much smaller number of independent structures in Eq. (2.17), recursive solution to Watson equations allow one to find all π's starting with (2.18). We give an example in Appendix A.2. All other multi-particle pentagons can be found analogously making use of the automatic solver in the accompanying notebook.

2.3. Mixed matrices

Last but not least, we address the case when both holes and (anti)fermions are present in the transition. We start with holes and antifermions, first, and then add fermions to the mix.

Namely, the N holes to $2N$ antifermion transitions,

$$P^{\boldsymbol{AB}|}{}_{\boldsymbol{C}}(\boldsymbol{u}|\boldsymbol{v}) = \langle \bar{\boldsymbol{\Psi}}_{\boldsymbol{C}}(\boldsymbol{v})|\mathcal{P}|\mathbf{h}^{\boldsymbol{AB}}(\boldsymbol{u})\rangle\,, \tag{2.21}$$

where the rapidity arrays are N, $\boldsymbol{u} = (u_1, \ldots, u_N)$, and $2N$, $\boldsymbol{v} = (v_1, \ldots, v_{2N})$, dimensional, respectively, and the sets of the SU(4) indices in the defining representation having the same lengths, $\boldsymbol{A} = (A_1, \ldots, A_N)$, $\boldsymbol{B} = (B_1, \ldots, B_N)$ and $\boldsymbol{C} = (C_1, \ldots, C_{2N})$. The above matrix element factorizes as before

$$P^{\boldsymbol{AB}|}{}_{\boldsymbol{C}}(\boldsymbol{u}|\boldsymbol{v}) = \Pi^{\boldsymbol{AB}|}{}_{\boldsymbol{C}}(\boldsymbol{u}|\boldsymbol{v})\, P_{\mathbf{h}|\boldsymbol{\Psi}}(\boldsymbol{u}|\boldsymbol{v})\,. \tag{2.22}$$

Here $P_{\mathbf{h}|\boldsymbol{\Psi}}(\boldsymbol{u}|\boldsymbol{v})$ admits again the form

$$P_{\mathbf{h}|\boldsymbol{\Psi}}(\boldsymbol{u}|\boldsymbol{v}) = \frac{\prod\limits_{i,j}^{N,2N} P_{\mathrm{h}|\Psi}(u_i|v_j)}{\prod\limits_{i>j}^{N} P_{\mathrm{h}|\mathrm{h}}(u_i|u_j)\prod\limits_{i<j}^{2N} P_{\Psi|\Psi}(v_i|v_j)}\,. \tag{2.23}$$

The decomposition of $\Pi^{\boldsymbol{AB}|}{}_{\boldsymbol{C}}(\boldsymbol{u}|\boldsymbol{v})$ into independent tensors is accomplished in the same manner as for the purely fermionic transitions discussed above, i.e., generating $2N!$ different pairings. However, this time one has to impose additional constraints for antisymmetry of N pairs of $\boldsymbol{A}$ and $\boldsymbol{B}$ indices. This yields a total number of $2N!/2^N$ independent structures,

$$\begin{aligned}&\Pi^{\boldsymbol{AB}|}{}_{\boldsymbol{C}}(\boldsymbol{u}|\boldsymbol{v}) \\ &\quad= \delta_{C_1}^{[A_1}\delta_{C_2}^{B_1]}\ldots\delta_{C_{2N-1}}^{[A_N}\delta_{C_{2N}}^{B_N]}\pi_1(\boldsymbol{u}|\boldsymbol{v}) + \cdots + \delta_{C_1}^{[A_N}\delta_{C_2}^{B_N]}\ldots\delta_{C_{2N-1}}^{[A_1}\delta_{C_{2N}}^{B_1]}\pi_{2N!/2^N}(\boldsymbol{u}|\boldsymbol{v}).\end{aligned} \tag{2.24}$$

As in the purely fermionic case, there are no closed mirror equations for the amplitude in question. So we will conjecture the twisted component again. It will take the form of the previous two cases, with a generalization to account for twice the number of rapidities on the top of the pentagon. Basically, we lump them up in nearest-neighbor pairs starting with the first position and double the number of rational factors in the numerator. Taking into account different values of helicity which result in half-integer imaginary shifts, we find

$$\begin{aligned}&\pi_{2N!/2^N}(\boldsymbol{u}|\boldsymbol{v}) \\ &= \frac{\prod\limits_{k_1=1}^{N-1}\prod\limits_{j_1=1}^{N-k_1}(u_{j_1}|v_{2k_1-1})_{-1/2}(u_{j_1}|v_{2k_1})_{-1/2}\prod\limits_{j_2=2}^{N}\prod\limits_{k_2=j_2}^{N-k_2}(u_{j_2}|v_{2N-2k_2+1})_{3/2}(u_{j_2}|v_{2N-2k_2+2})_{3/2}}{\prod\limits_{j_1=1}^{N-1}\prod\limits_{k_1=j_1+1}^{N-1}(u_{j_1}|u_{k_1})_{-1}(u_{j_1}|u_{k_1})_{-2}\prod\limits_{j_1=1}^{2N-1}\prod\limits_{k_1=j_1+1}^{2N-1}(v_{j_1}|v_{k_1})_1}.\end{aligned} \tag{2.25}$$

The remaining functions in the tensor decomposition (2.24) arise from this by repeated use of $(2N-1)$ final-state Watson equations involving fermionic S-matrices of the previous subsection. This is demonstrated on a simple example in Appendix A.3, with higher particle number cases deferred to the accompanying file.

Finally, it is left to consider all types of excitations with isotopic indices residing on the contour. The simplest case, that is the basis for all other possibilities, is of N fermions with

rapidities $\boldsymbol{u} = (u_1, \ldots, u_N)$ and M holes with rapidities $\boldsymbol{v} = (v_1, \ldots, v_M)$ on the bottom and $N + 2M$ antifermions with rapidities $\boldsymbol{w} = (w_1, \ldots, w_{N+2M})$ on the top,

$$P^{\boldsymbol{ABC}|}{}_{\boldsymbol{D}}(\boldsymbol{u}, \boldsymbol{v}|\boldsymbol{w}) = \langle \bar{\boldsymbol{\Psi}}_{\boldsymbol{D}}(\boldsymbol{w})|\mathcal{P}|\boldsymbol{\Psi}^{\boldsymbol{A}}(\boldsymbol{u})\mathbf{h}^{\boldsymbol{BC}}(\boldsymbol{v})\rangle\,. \tag{2.26}$$

Again the SU(4) matrix in the factorized expression

$$P^{\boldsymbol{ABC}|}{}_{\boldsymbol{D}}(\boldsymbol{u}, \boldsymbol{v}|\boldsymbol{w}) = \Pi^{\boldsymbol{ABC}|}{}_{\boldsymbol{D}}(\boldsymbol{u}, \boldsymbol{v}|\boldsymbol{w})\, P_{\boldsymbol{\Psi h}|\boldsymbol{\Psi}}(\boldsymbol{u}, \boldsymbol{v}|\boldsymbol{w}) \tag{2.27}$$

admits the form

$$\begin{aligned}
&\Pi^{\boldsymbol{ABC}|}{}_{\boldsymbol{D}}(\boldsymbol{u}, \boldsymbol{v}|\boldsymbol{w}) \\
&= \delta^{A_1}_{D_1} \ldots \delta^{A_N}_{D_N} \delta^{[B_1}_{D_{N+1}} \delta^{C_1]}_{D_{N+2}} \ldots \delta^{[B_M}_{D_{N+2M-1}} \delta^{C_M]}_{D_{N+2M}} \pi_1(\boldsymbol{u}, \boldsymbol{v}|\boldsymbol{w}) + \ldots \\
&+ \delta^{A_1}_{D_{N+2M}} \ldots \delta^{A_N}_{D_{2M+1}} \delta^{[B_1}_{D_{2M}} \delta^{C_1]}_{D_{2M-1}} \ldots \delta^{[B_M}_{D_2} \delta^{C_M]}_{D_1} \pi_{(N+2M)!/2^M}(\boldsymbol{u}, \boldsymbol{v}|\boldsymbol{w})\,.
\end{aligned} \tag{2.28}$$

The dynamical term has the same structure as earlier in terms of one-to-one pentagons

$$P_{\boldsymbol{\Psi h}|\boldsymbol{\Psi}}(\boldsymbol{u}, \boldsymbol{v}|\boldsymbol{w}) = \frac{\prod\limits_{i,j}^{N,N+2M} P_{\Psi|\Psi}(u_i|w_j) \prod\limits_{i,j}^{M,N+2M} P_{\mathrm{h}|\Psi}(v_i|w_j)}{\prod\limits_{i<j}^{N+2M} P_{\Psi|\bar{\Psi}}(w_i|w_j) \prod\limits_{i>j}^{N} P_{\Psi|\bar{\Psi}}(u_i|u_j) \prod\limits_{i>j}^{M} P_{\mathrm{h}|\mathrm{h}}(v_i|v_j) \prod\limits_{i,j}^{M,N} P_{\mathrm{h}|\Psi}(v_i|u_j)}\,. \tag{2.29}$$

The twisted function in the matrix part now reads

$$\pi_{(N+2M)!/2^M}(\boldsymbol{u}, \boldsymbol{v}|\boldsymbol{w}) = \frac{\mathcal{N}_1(\boldsymbol{u}, \boldsymbol{v}|\boldsymbol{w})\mathcal{N}_2(\boldsymbol{u}, \boldsymbol{v}|\boldsymbol{w})}{\mathcal{D}(\boldsymbol{u}, \boldsymbol{v}|\boldsymbol{w})}\,, \tag{2.30}$$

where

$$\begin{aligned}
\mathcal{N}_1(\boldsymbol{u}, \boldsymbol{v}|\boldsymbol{w}) &= \prod_{k=1}^{M} \prod_{j=N+1}^{N+M-k} (v_j|w_{2k-1})_{-1/2} (v_j|w_{2k})_{-1/2} \prod_{j=1}^{N} (u_j|w_{2k-1})_0 (u_j|w_{2k})_0 \\
&\times \prod_{k=2M+1}^{N+2M-1} \prod_{j=N+1}^{N+2M-k} (v_j|w_k)_{-1/2} \prod_{j=1}^{N} (u_j|w_k)_0\,,
\end{aligned} \tag{2.31}$$

$$\begin{aligned}
\mathcal{N}_2(\boldsymbol{u}, \boldsymbol{v}|\boldsymbol{w}) &= \prod_{j=0}^{N-1} \prod_{k=j}^{N-2} (u_{k+2}|w_{N+2M-j})_1 \prod_{k=N-1}^{N+M-2} (v_{k+2}|w_{N+2M-j})_{3/2} \\
&\times \prod_{j=0}^{M-2} \prod_{k=j+N}^{N+M-2} (v_{k+2}|w_{2M-1-2j})_{3/2} (v_{k+2}|w_{2M-2j})_{3/2}\,,
\end{aligned} \tag{2.32}$$

$$\begin{aligned}
\mathcal{D}(\boldsymbol{u}, \boldsymbol{v}|\boldsymbol{w}) &= \prod_{j<k=2}^{N} (u_j|u_k)_{-1} \prod_{j<k=2}^{M} (v_j|v_k)_{-1} (v_j|v_k)_{-2} \\
&\times \prod_{j=1}^{N} \prod_{k=1}^{M} (u_j|v_k)_{-3/2} \prod_{j<k=2}^{N+2M} (w_j|w_k)_1\,.
\end{aligned} \tag{2.33}$$

This is demonstrated in Fig. 4.

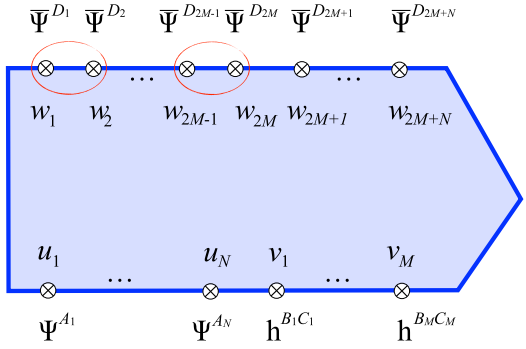

Fig. 4. Distribution of excitations on the mixed pentagon. The rapidities of the first $2M$ antifermions on the top are lumped in pairs such that the twisted structure follows the same pattern as purely hole/fermion on up to different shift assignments.

These results are all one needs to extract other singlet pentagon transitions which are allowed by quantum numbers, namely, by sending pairs of (conjugate) hole (fermion and anifermion) as well as quartets of (anti)fermionic rapidities to infinity. The origin for this limiting procedure is discussed in Sect. 4 below.

3. Moving excitations around

To obtain non-diagonal transitions, i.e., involving different number of excitations on the top and the bottom or all of them residing on one side, we have to move particles around the contour. For scalars, it is straightforward and is accomplished with the help of the double Wick rotation already used in the derivation of the Mirror equations in Sect. 2.1.1. We will be interested here in the creation form factor but other cases can be obtained analogously. Starting with the N-to-N transition (2.2), every time we get a hole from the bottom to the top side of the pentagon, we acquire one power of $R_{\mathrm{h}|\mathrm{h}}$. When we move all excitations from the bottom to the top, we deduce the form factor in question

$$P^{0|\boldsymbol{I}\boldsymbol{J}}(0|\boldsymbol{u},\boldsymbol{v}) = P^{\bar{\boldsymbol{I}}|\boldsymbol{J}}(\bar{\boldsymbol{u}}^{2\gamma}|\boldsymbol{v}) = \Pi^{0|\boldsymbol{I}\boldsymbol{J}}(0|\boldsymbol{u},\boldsymbol{v})P_{0|\mathbf{h}}(0|\boldsymbol{u},\boldsymbol{v})\,, \tag{3.1}$$

where we used barred notations for reversed order of rapidities $\bar{\boldsymbol{u}} = (u_N,\dots,u_1)$ and O(6) indices $\bar{\boldsymbol{I}} = (I_N,\dots,I_1)$. Here we stripped the dynamical component from the emerging rational prefactors,

$$P_{0|\mathbf{h}}(0|\boldsymbol{u},\boldsymbol{v}) = \frac{1}{\prod\limits_{i,j}^{N} P_{\mathrm{h}|\mathrm{h}}(u_i|v_j)\prod\limits_{i<j}^{N} P_{\mathrm{h}|\mathrm{h}}(v_i|v_j)P_{\mathrm{h}|\mathrm{h}}(u_i|u_j)}\,, \tag{3.2}$$

and shifting them into the SU(4) matrix, which reads as a result

$$\Pi^{0|\boldsymbol{I}\boldsymbol{J}}(0|\boldsymbol{u},\boldsymbol{v}) = \frac{\Pi^{\bar{\boldsymbol{I}}|\boldsymbol{J}}(\bar{\boldsymbol{u}}+2i|\boldsymbol{v})}{\prod\limits_{i,j}^{N}(u_i|v_j)_1(u_i|v_j)_2} \tag{3.3}$$

in terms of the one determined for the transition amplitude (2.4). For instance, the matrix part of the two-hole creation form factor is

$$\Pi^{0|I_1,I_2}(0|\boldsymbol{u}) = \delta^{I_1 I_2} R_{\rm hh}(u_1,u_2)\,, \tag{3.4}$$

with $R_{\rm hh}(u_1,u_2)$ given in Eq. (2.6).

Fermions, on the other hand, do not have a one-particle mirror transformation. However, from the point of view of the matrix rational prefactor, the modification of changing the tensor as one "moves" fermions around should not be drastic. We found a useful mnemonic rule, which results in producing a rational factor every time we pass the fermion from the initial to the final state

$$R_{\Psi\Psi}(u,v) = \frac{1}{(u|v)_2}\,. \tag{3.5}$$

Recall that for scalars, the denominator of the rational factor was $(u|v)_1(u|v)_2$, see Eq. (2.6), while for gluons there will be none, i.e., it equals one. The fermion is somewhat intermediate between the two and thus was conjectured to have just one factor of particle rapidities. This is analogous to the consideration in Ref. [6] where a relation between single-fermion transition and two-fermion form factor was found using similar arguments. The creation form factor of N fermions and N antifermions is

$$P^{0|\boldsymbol{A}}{}_{\boldsymbol{B}}(0|\boldsymbol{u},\boldsymbol{v}) = \Pi^{0|\boldsymbol{A}}{}_{\boldsymbol{B}}(0|\boldsymbol{u},\boldsymbol{v})\,P_{0|\boldsymbol{\Psi}}(0|\boldsymbol{u},\boldsymbol{v})\,, \tag{3.6}$$

where the dynamical part,

$$P_{0|\boldsymbol{\Psi}}(0|\boldsymbol{u},\boldsymbol{v}) = \frac{1}{\prod\limits_{i,j}^{N} P_{\Psi|\Psi}(u_i|v_j)\prod\limits_{i<j}^{N} P_{\Psi|\Psi}(v_i|v_j)\prod\limits_{i<j}^{N} P_{\Psi|\Psi}(u_i|u_j)}\,, \tag{3.7}$$

is accompanied by the matrix one

$$\Pi^{0|\boldsymbol{A}}{}_{\boldsymbol{B}}(0|\boldsymbol{u},\boldsymbol{v}) = \frac{\Pi^{\bar{A}|}{}_{\boldsymbol{B}}(\bar{\boldsymbol{u}}+2i|\boldsymbol{v})}{\prod\limits_{i,j}^{N}(u_i|v_j)_2}\,, \tag{3.8}$$

similar to the rules for the hole excitations.

For the pentagon transitions involving both fermions and holes, one has to add the following mirror transformation

$$P_{\rm h|\Psi}(u^{2\gamma}|v) = \frac{R_{\rm h\Psi}(u,v)}{P_{\rm h|\Psi}(u|v)}\,, \qquad R_{\rm h\Psi}(u,v) = \frac{1}{(u|v)_{3/2}}\,. \tag{3.9}$$

Then the creation form factor of N scalars and $2N$ antifermions is

$$P^{0|\boldsymbol{AB}}{}_{\boldsymbol{C}}(0|\boldsymbol{u},\boldsymbol{v}) = \Pi^{0|\boldsymbol{AB}}{}_{\boldsymbol{C}}(0|\boldsymbol{u},\boldsymbol{v})\,P_{0|\mathbf{h}\boldsymbol{\Psi}}(0|\boldsymbol{u},\boldsymbol{v})\,, \tag{3.10}$$

where

$$P_{0|\mathbf{h}\boldsymbol{\Psi}}(0|\boldsymbol{u},\boldsymbol{v}) = \frac{1}{\prod\limits_{i,j}^{N,2N} P_{\rm h|\Psi}(u_i|v_j)\prod\limits_{i<j}^{2N} P_{\Psi|\Psi}(v_i|v_j)\prod\limits_{i<j}^{N} P_{\rm h|h}(u_i|u_j)}\,, \tag{3.11}$$

and

$$\Pi^{0|\boldsymbol{AB}}{}_{\boldsymbol{C}}(0|\boldsymbol{u},\boldsymbol{v}) = \frac{\Pi^{\bar{A}\bar{B}|}{}_{\boldsymbol{C}}(\bar{\boldsymbol{u}}+2i|\boldsymbol{v})}{\prod\limits_{i,j}^{N}(u_i|v_j)_{3/2}}\,. \tag{3.12}$$

Finally, for the pentagons with all excitations present on its top, using the rules advocated for the fermions and mirror transformation for the holes, we find

$$P^{0|\boldsymbol{BCA}}{}_{\boldsymbol{D}}(0|\boldsymbol{v},\boldsymbol{u},\boldsymbol{w}) = \Pi^{0|\boldsymbol{BCA}}{}_{\boldsymbol{D}}(0|\boldsymbol{v},\boldsymbol{u},\boldsymbol{w})\, P_{0|\mathbf{h}\bar{\Psi}\Psi}(0|\boldsymbol{v},\boldsymbol{u},\boldsymbol{w})\,, \tag{3.13}$$

where the dynamical component is

$$\begin{aligned} P_{0|\mathbf{h}\bar{\Psi}\Psi}(0|\boldsymbol{v},\boldsymbol{u},\boldsymbol{w}) = {} & \frac{1}{\prod\limits_{i<j}^{N+2M} P_{\Psi|\bar{\Psi}}(w_i|w_j) \prod\limits_{i<j}^{N} P_{\Psi|\bar{\Psi}}(u_i|u_j) \prod\limits_{i<j}^{M} P_{\mathrm{h}|\mathrm{h}}(v_i|v_j)} \\ & \times \frac{1}{\prod\limits_{i,j}^{M,N} P_{\mathrm{h}|\Psi}(v_i|u_j) \prod\limits_{i,j}^{N,N+2M} P_{\Psi|\Psi}(u_i|w_j) \prod\limits_{i,j}^{M,N+2M} P_{\mathrm{h}|\Psi}(v_i|w_j)}\,, \end{aligned} \tag{3.14}$$

while the matrix part reads

$$\Pi^{0|\boldsymbol{BCA}}{}_{\boldsymbol{D}}(0|\boldsymbol{v},\boldsymbol{u},\boldsymbol{w}) = \frac{\Pi^{\boldsymbol{ABC}|}{}_{\boldsymbol{D}}(\bar{\boldsymbol{u}}+2i,\bar{\boldsymbol{v}}+2i|\boldsymbol{w})}{\prod\limits_{i,j}^{N,N+2M}(u_i|w_j)_2 \prod\limits_{i,j}^{M,N+2M}(v_i|w_j)_{3/2}}\,. \tag{3.15}$$

4. Non-singlet pentagons

Having discussed the singlet pentagons, we are ready to discuss the non-singlet, or charged, transitions. We will not need to address anew equations they obey. We will provide expressions for these making use of the fact that fermions at zero momentum become supersymmetry generators [21]. While for the dynamical component the zero-momentum limit has to be taken on the small fermion sheet [4], where $p=0$ corresponds to $u\to\infty$, for the rational matrix this can be achieved without performing the analytical continuation and simply taking the infinite-rapidity limit. This allows one to find the **4** (and $\bar{\mathbf{4}}$) pentagons, or rather their tensor structures

$$[\Pi^{A_1}]^{\cdots|}{}_{\ldots}(\boldsymbol{u}'|\boldsymbol{v}) = \lim_{u_1\to\infty} u_1^{\#}\Pi^{A_1\cdots|}{}_{\ldots}(\boldsymbol{u}|\boldsymbol{v})\,, \tag{4.1}$$

where $\boldsymbol{u}'$ is obtained from $\boldsymbol{u}$ by removing the rapidity associated with the SU(4) index A_1, i.e., $\boldsymbol{u}'=\boldsymbol{u}\backslash u_1=(u_2,\ldots,u_N)$ and # is the exponent of the leading power behavior. The latter depends on in- and out-states involved in the transition. In the current study it was empirically found on case-by-case basis. It should be possible to derive its generic form for an arbitrary transition, however, we have not succeeded in accomplishing this at the moment. One can take the limit with respect to any rapidity of fermions involved, yielding the pentagon charged with respect to the corresponding index. Identical considerations give the $\bar{\mathbf{4}}$-pentagon when one sends corresponding anti-fermion rapidity to infinity or equivalently three fermionic ones.

From the point of view of the matrix structure, two fermions with antisymmetrized indices are identical to the hole insertion. Therefore, one can extract pentagons charged with respect to the **6** of SU(4) by sending corresponding hole rapidity to infinity,

$$[\Pi^{I_1}]^{\cdots}{}_{\ldots}(\boldsymbol{u}'|\boldsymbol{v}) = \lim_{u_1\to\infty} u_1^{\#}\Pi^{I_1\cdots}{}_{\ldots}(\boldsymbol{u}|\boldsymbol{v})\,, \tag{4.2}$$

where $\boldsymbol{u}'$ is the same as above. Conversion back to the indices in the (anti)fundamental representation can be achieved as discussed in the Footnote 1. Of course, in all cases it is irrelevant whether we pick up an excitation sent to infinite rapidity in the initial or final state.

With expressions in hand for (2.16), the pentagons involving quartets of anti- and fermions arise from by taking the rapidities of conjugate excitations to infinity, e.g.,

$$\begin{aligned}&\varepsilon_{B_1B_2B_3B_4}\Pi^{A_1A_2A_3A_4|0}(u_1,u_2,u_3,u_4|0)\\&=\lim_{v\to\infty}v^{\#}\Pi^{A_1A_2A_3A_4|}{}_{B_1B_2B_3B_4}(u_1,u_2,u_3,u_4|v,v,v,v)\,,\end{aligned}\tag{4.3}$$

where

$$\Pi^{A_1A_2A_3A_4|0}(u_1,u_2,u_3,u_4|0)=\frac{\varepsilon^{A_1A_2A_3A_4}}{\prod_{i<j}^{4}(u_i|u_j)_{-1}}\,.\tag{4.4}$$

Another example is demonstrated in Appendix A.1.

5. Gluing up polygons

The known matrix form of pentagon transitions allows one to immediately construct higher polygons. We will address the scalars only as a case of study. It clearly demonstrates the gluing procedure without the complication of dealing with different flux-tube excitations and their SU(4) indices. The contraction of SU(4) tensors is not a problem for symbolic manipulations but the cumbersome form of the output prevents us from displaying final results explicitly in the paper. Thus they are left for the accompanying notebook.

The contribution of $N_{\rm h}$-hole state propagating in the N-gon is

$$\begin{aligned}W_N^{N_{\rm h}}=\frac{1}{N_{\rm h}!}\int d\boldsymbol{\mu}_{\rm h}\,\Pi^{0|\boldsymbol{I}^{(1)}}(0|\boldsymbol{u}^{(1)})\left[\prod_{\ell=1}^{N-6}\Pi^{\bar{\boldsymbol{I}}^{(\ell)}|\boldsymbol{I}^{(\ell+1)}}(-\boldsymbol{u}^{(\ell)}|\boldsymbol{u}^{(\ell+1)})\right]\Pi^{0|\bar{\boldsymbol{I}}^{(N-5)}}(0|\bar{\boldsymbol{u}}^{(N-5)})\\\times P_{0|\mathbf{h}}(0|\boldsymbol{u}^{(1)})\left[\prod_{\ell=1}^{N-6}P_{\mathbf{h}|\mathbf{h}}(-\boldsymbol{u}^{(\ell)}|\boldsymbol{u}^{(\ell+1)})\right]P_{0|\mathbf{h}}(0|\bar{\boldsymbol{u}}^{(N-5)})\,,\end{aligned}$$

where the integration measure is conventionally determined by (here for $\mathrm{p}=\mathrm{h}$)

$$d\boldsymbol{\mu}_{\rm h}=\prod_{i=1}^{N_{\rm h}}\prod_{\ell=1}^{N-5}d\mu_{\rm h}(u_i^{(\ell)})\,,\qquad d\mu_{\rm p}(u^{(\ell)})=\frac{du}{2\pi}\mu(u_\ell)\mathrm{e}^{-\tau_\ell E_{\rm p}(u^{(\ell)})+i\sigma_\ell p_{\rm p}(u^{(\ell)})}\,,\tag{5.1}$$

with propagation exponents included. Obviously, for the MHV polygon, the creation and annihilation form factors are singlets and have an even number of holes. While for the NMHV case, the number of scalars is odd since the pentagon operator itself is a sextet of SU(4). The corresponding index gets contracted directly between the top and bottom as all intermediate pentagons are charge-free. The three-particle case is displayed explicitly in Eq. (A.19) of Appendix A.1. Here and above we used the relation between the creation/annihilation form factors

$$P^{\boldsymbol{I}|0}(\boldsymbol{u}|0)=P^{0|\boldsymbol{I}}(0|-\boldsymbol{u})\,.\tag{5.2}$$

The contraction of SU(4) matrices can easily be done but results in extremely long expressions due to the factorial growth of the number of functions involved, except, of course, for the two-hole case which yields a product of $N-6$ factors $(6\pi_1+\pi_2+\pi_3)$ with arguments as shown in Eq. (5.1). With these results in hand, one can extend the consideration of Refs. [15,22,23] dedicated to the hexagon to the analysis of collinear expansion of any superloop at strong coupling.

To date, there are no explicit results available in the literature for generic number of excitations for polygons with more than six sides. However, we can test our expressions for tensor functions against the matrix part of the hexagon proposed in Refs. [15,16]. These consistency cross checks are performed in the accompanying notebook for a number of examples with excitations less than ten, the main obstacle for reaching higher numbers being the highly time consuming extraction of the rational function from the integral representation in the above papers by taking the residues of the integrand as the number of auxiliary rapidities grows pretty fast.

6. Conclusions

In this paper, we developed a constructive method for determination of the internal symmetry group structure of multi-particle (non)singlet pentagons which enter as fundamental building blocks in the operator product expansion of scattering amplitudes in maximally supersymmetric Yang–Mills theory. The formalism is based upon analytical solution of a system of the Mirror and Watson equations obeyed by the corresponding transitions. Their recursive solution reduces all functions accompanying independent tensor structures to just one. The latter was conjectured to admit a rational form in terms rapidities of flux-tube excitations and verified a number of tests, which convince us in its correctness. With this final ingredient in place, the problem of near collinear expansion of scattering amplitudes at any value of the coupling could be viewed as completed. However, it would nevertheless be highly important to deduce multiple integral representation for contraction of pentagon tensors as they enter the actual scattering amplitudes, generalizing the earlier consideration for the hexagon [16].

Acknowledgements

This research was supported by the U.S. National Science Foundation under the grants PHY-1068286 and PHY-1403891.

Appendix A. Explicit examples

Let us provide a few examples for each representative case.

A.1. Holes

We give the simplest example first, the two-to-two hole transition. The three independent matrix structures are parametrized by two sets of rapidities $\boldsymbol{u} = (u_1, u_2)$ and $\boldsymbol{v} = (v_1, v_2)$ for the initial and final states, respectively. The starting point of the recursion is

$$\pi_3(\boldsymbol{u}|\boldsymbol{v}) = \frac{(u_1|v_1)_0(u_2|v_2)_1}{(u_1|u_2)_{-1}(v_1|v_2)_1}\,, \tag{A.1}$$

with the other two found from the Watson and Mirror equations

$$\pi_2(\boldsymbol{u}|\boldsymbol{v}) = \frac{\pi_3(\boldsymbol{u}|v_2, v_1) - s^{(2)}_{\rm hh}(v_1, v_2)\pi_3(\boldsymbol{u}|\boldsymbol{v})}{s^{(1)}_{\rm hh}(v_1, v_2)}\,, \tag{A.2}$$

$$\pi_1(\boldsymbol{u}|\boldsymbol{v}) = \frac{(u_1|v_1)_0(u_1|v_1)_{-1}(u_2|v_2)_1(u_2|v_2)_2}{(u_1|u_2)_{-1}(u_1|u_2)_{-2}(v_1|v_2)_1(v_1|v_2)_2}\pi_2(v_1 + 2i, u_1|v_2, u_2 + 3i)\,, \tag{A.3}$$

respectively. Substituting the explicit expressions for scattering matrix, we find an agreement with the result of Ref. [5] for the case at hand.

Next, for three-to-three scalar transition parametrized by rapidity arrays $\boldsymbol{u} = (u_1, u_2, u_3)$ and $\boldsymbol{v} = (v_1, v_2, v_3)$ for the initial and final state, respectively, the "boundary value" is set by

$$\pi_{15}(\boldsymbol{u}|\boldsymbol{v}) = \frac{(u_1|v_1)_0(u_2|v_1)_0(u_1|v_2)_0(u_3|v_2)_1(u_2|v_3)_1(u_3|v_3)_1}{(u_1|u_2)_{-1}(u_1|u_3)_{-1}(u_2|u_3)_{-1}(v_1|v_2)_1(v_1|v_3)_1(v_2|v_3)_1}\,. \tag{A.4}$$

Then, one can immediately find with the help of a Mathematica routine in the accompanying notebook,

$$\pi_{14}(\boldsymbol{u}|\boldsymbol{v}) = \frac{\pi_{15}(\boldsymbol{u}|v_2, v_1, v_3) - s^{(2)}_{\rm hh}(v_1, v_2)\pi_{15}(\boldsymbol{u}|\boldsymbol{v})}{s^{(1)}_{\rm hh}(v_1, v_2)}\,, \tag{A.5}$$

$$\pi_{12}(\boldsymbol{u}|\boldsymbol{v}) = \frac{\pi_{15}(\boldsymbol{u}|v_1, v_3, v_2) - s^{(2)}_{\rm hh}(v_2, v_3)\pi_{15}(\boldsymbol{u}|\boldsymbol{v})}{s^{(1)}_{\rm hh}(v_2, v_3)}\,, \tag{A.6}$$

$$\pi_{11}(\boldsymbol{u}|\boldsymbol{v}) = \frac{\pi_{14}(\boldsymbol{u}|v_1, v_3, v_2) - s^{(2)}_{\rm hh}(v_2, v_3)\pi_{14}(\boldsymbol{u}|\boldsymbol{v})}{s^{(1)}_{\rm hh}(v_2, v_3)}\,, \tag{A.7}$$

$$\pi_{9}(\boldsymbol{u}|\boldsymbol{v}) = \frac{\pi_{12}(\boldsymbol{u}|v_2, v_1, v_3) - s^{(2)}_{\rm hh}(v_1, v_2)\pi_{12}(\boldsymbol{u}|\boldsymbol{v})}{s^{(1)}_{\rm hh}(v_1, v_2)}\,, \tag{A.8}$$

$$\pi_{8}(\boldsymbol{u}|\boldsymbol{v}) = \frac{\pi_{11}(\boldsymbol{u}|v_2, v_1, v_3) - s^{(2)}_{\rm hh}(v_1, v_2)\pi_{11}(\boldsymbol{u}|\boldsymbol{v})}{s^{(1)}_{\rm hh}(v_1, v_2)}\,, \tag{A.9}$$

$$\begin{aligned}
&\pi_{5}(\boldsymbol{u}|\boldsymbol{v}) \\
&= \frac{(u_2|u_3)_{-1}(u_2|u_3)_{-2}(u_1|v_1)_0(u_1|v_1)_{-1}(u_1|v_2)_0(u_1|v_2)_{-1}(u_2|v_3)_1(u_2|v_3)_2(u_3|v_3)_1(u_3|v_3)_2}{(u_1|u_2)_{-1}(u_1|u_2)_{-2}(u_2|u_3)_{-1}(u_2|u_3)_{-2}(u_1|u_3)_{-1}(u_1|u_3)_{-2}(v_1|v_3)_1(v_1|v_3)_2(v_2|v_3)_1(v_2|v_3)_2} \\
&\times \pi_{14}(v_2 + 2i, v_1 + 2i, u_1|v_3, u_3 + 3i, u_2 + 3i)\,,
\end{aligned} \tag{A.10}$$

$$\begin{aligned}
\pi_{13}(\boldsymbol{u}|\boldsymbol{v}) &= \frac{(u_1|v_1)_0(u_1|v_1)_{-1}(u_2|v_1)_0(u_2|v_1)_{-1}(u_3|v_2)_1(u_3|v_2)_2(u_3|v_3)_1(u_3|v_3)_2}{(u_2|u_3)_{-1}(u_2|u_3)_{-2}(u_1|u_3)_{-1}(u_1|u_3)_{-2}(v_1|v_2)_1(v_1|v_2)_2(v_1|v_3)_1(v_1|v_3)_2} \\
&\times \pi_{8}(v_1 + 2i, u_1, u_2|v_2, v_3, u_3 + 3i)\,,
\end{aligned} \tag{A.11}$$

$$\begin{aligned}
&\pi_{1}(\boldsymbol{u}|\boldsymbol{v}) \\
&= \frac{(u_2|u_3)_{-1}(u_2|u_3)_{-2}(u_1|v_1)_0(u_1|v_1)_{-1}(u_1|v_2)_0(u_1|v_2)_{-1}(u_2|v_3)_1(u_2|v_3)_2(u_3|v_3)_1(u_3|v_3)_2}{(u_1|u_2)_{-1}(u_1|u_2)_{-2}(u_2|u_3)_{-1}(u_2|u_3)_{-2}(u_1|u_3)_{-1}(u_1|u_3)_{-2}(v_1|v_3)_1(v_1|v_3)_2(v_2|v_3)_1(v_2|v_3)_2} \\
&\times \pi_{8}(v_2 + 2i, v_1 + 2i, u_1|v_3, u_3 + 3i, u_2 + 3i)\,,
\end{aligned} \tag{A.12}$$

$$\begin{aligned}
\pi_{10}(\boldsymbol{u}|\boldsymbol{v}) &= \frac{(u_1|v_1)_0(u_1|v_1)_{-1}(u_2|v_1)_0(u_2|v_1)_{-1}(u_3|v_2)_1(u_3|v_2)_2(u_3|v_3)_1(u_3|v_3)_2}{(u_2|u_3)_{-1}(u_2|u_3)_{-2}(u_1|u_3)_{-1}(u_1|u_3)_{-2}(v_1|v_2)_1(v_1|v_2)_2(v_1|v_3)_1(v_1|v_3)_2} \\
&\times \pi_{11}(v_1 + 2i, u_1, u_2|v_2, v_3, u_3 + 3i)\,,
\end{aligned} \tag{A.13}$$

$$\begin{aligned}
&\pi_{2}(\boldsymbol{u}|\boldsymbol{v}) \\
&= \frac{(u_2|u_3)_{-1}(u_2|u_3)_{-2}(u_1|v_1)_0(u_1|v_1)_{-1}(u_1|v_2)_0(u_1|v_2)_{-1}(u_2|v_3)_1(u_2|v_3)_2(u_3|v_3)_1(u_3|v_3)_2}{(u_1|u_2)_{-1}(u_1|u_2)_{-2}(u_2|u_3)_{-1}(u_2|u_3)_{-2}(u_1|u_3)_{-1}(u_1|u_3)_{-2}(v_1|v_3)_1(v_1|v_3)_2(v_2|v_3)_1(v_2|v_3)_2} \\
&\times \pi_{11}(v_2 + 2i, v_1 + 2i, u_1|v_3, u_3 + 3i, u_2 + 3i)\,,
\end{aligned} \tag{A.14}$$

$$\pi_6(\boldsymbol{u}|\boldsymbol{v}) = \frac{(u_1|v_1)_0(u_1|v_1)_{-1}(u_2|v_1)_0(u_2|v_1)_{-1}(u_3|v_2)_1(u_3|v_2)_2(u_3|v_3)_1(u_3|v_3)_2}{(u_2|u_3)_{-1}(u_2|u_3)_{-2}(u_1|u_3)_{-1}(u_1|u_3)_{-2}(v_1|v_2)_1(v_1|v_2)_2(v_1|v_3)_1(v_1|v_3)_2} \times \pi_9(v_1+2i, u_1, u_2|v_2, v_3, u_3+3i)\,, \tag{A.15}$$

$$\pi_4(\boldsymbol{u}|\boldsymbol{v}) = \frac{(u_2|u_3)_{-1}(u_2|u_3)_{-2}(u_1|v_1)_0(u_1|v_1)_{-1}(u_1|v_2)_0(u_1|v_2)_{-1}(u_2|v_3)_1(u_2|v_3)_2(u_3|v_3)_1(u_3|v_3)_2}{(u_1|u_2)_{-1}(u_1|u_2)_{-2}(u_2|u_3)_{-1}(u_2|u_3)_{-2}(u_1|u_3)_{-1}(u_1|u_3)_{-2}(v_1|v_3)_1(v_1|v_3)_2(v_2|v_3)_1(v_2|v_3)_2} \times \pi_9(v_2+2i, v_1+2i, u_1|v_3, u_3+3i, u_2+3i)\,, \tag{A.16}$$

$$\pi_7(\boldsymbol{u}|\boldsymbol{v}) = \frac{\pi_{10}(\boldsymbol{u}|v_2, v_1, v_3) - s^{(2)}_{\rm hh}(v_1, v_2)\pi_{10}(\boldsymbol{u}|\boldsymbol{v})}{s^{(1)}_{\rm hh}(v_1, v_2)}\,, \tag{A.17}$$

$$\pi_3(\boldsymbol{u}|\boldsymbol{v}) = \frac{\pi_2(\boldsymbol{u}|v_1, v_3, v_2) - s^{(2)}_{\rm hh}(v_2, v_3)\pi_2(\boldsymbol{u}|\boldsymbol{v})}{s^{(1)}_{\rm hh}(v_2, v_3)}\,. \tag{A.18}$$

In Sect. 5 dedicated to the construction of higher polygons, we need an expression for the charged pentagon creation form factor. As we explained in Sect. 3, all non-singlet pentagons can be found from the singlet ones. For the case at hand, we use the $2 \to 2$ hole transition and move all excitations to the top according to Eq. (4.2) and then, sending one of the rapidities there to infinity, we find, making use of the result (3.3),

$$[\Pi^I]^{0|I_1I_2I_3}(0|\boldsymbol{v}) = \delta^{I_1I_2}\delta^{I_3I}\,R^{(1)}_{\rm hhh}(\boldsymbol{v}) + \delta^{I_2I_3}\delta^{I_1I}\,R^{(2)}_{\rm hhh}(\boldsymbol{v}) + \delta^{I_1I_3}\delta^{I_2I}\,R^{(3)}_{\rm hhh}(\boldsymbol{v})\,. \tag{A.19}$$

Here

$$R^{(1)}_{\rm hhh}(\boldsymbol{v}) = \frac{(v_1|v_3)_3}{(v_1|v_2)_1(v_1|v_2)_2(v_1|v_3)_1(v_1|v_3)_2(v_2|v_3)_1}\,, \tag{A.20}$$

$$R^{(2)}_{\rm hhh}(\boldsymbol{v}) = \frac{(v_1|v_3)_{-3}}{(v_1|v_2)_1(v_2|v_3)_1(v_2|v_3)_2(v_1|v_3)_1(v_1|v_3)_2}\,, \tag{A.21}$$

$$R^{(3)}_{\rm hhh}(\boldsymbol{v}) = -\frac{1}{(v_1|v_2)_1(v_1|v_3)_1(v_1|v_3)_2(v_2|v_3)_1}\,. \tag{A.22}$$

Pentagons and form factors with larger number of particles are found in a similar manner.

A.2. Fermions

For the transition of three fermions with rapidities $\boldsymbol{u} = (u_1, u_2, u_3)$ to three antifermions with $\boldsymbol{v} = (v_1, v_2, v_3)$, we have

$$\pi_6(\boldsymbol{u}|\boldsymbol{v}) = \frac{(u_1|v_1)_0(u_2|v_1)_0(u_1|v_2)_0(u_3|v_2)_1(u_2|v_3)_1(u_3|v_3)_1}{(u_1|u_2)_{-1}(u_1|u_3)_{-1}(u_2|u_3)_{-1}(v_1|v_2)_1(v_1|v_3)_1(v_2|v_3)_1}\,, \tag{A.23}$$

and the rest are found from Watson equations

$$\pi_5(\boldsymbol{u}|\boldsymbol{v}) = \frac{\pi_6(\boldsymbol{u}|v_2, v_1, v_3) - s^{(2)}_{\Psi\Psi}(v_1, v_2)\pi_6(\boldsymbol{u}|\boldsymbol{v})}{s^{(1)}_{\Psi\Psi}(v_1, v_2)}\,, \tag{A.24}$$

$$\pi_4(\boldsymbol{u}|\boldsymbol{v}) = \frac{\pi_6(\boldsymbol{u}|v_1, v_3, v_2) - s^{(2)}_{\Psi\Psi}(v_2, v_3)\pi_6(\boldsymbol{u}|\boldsymbol{v})}{s^{(1)}_{\Psi\Psi}(v_2, v_3)}\,, \tag{A.25}$$

$$\pi_3(\boldsymbol{u}|\boldsymbol{v}) = \frac{\pi_5(\boldsymbol{u}|v_1, v_3, v_2) - s^{(2)}_{\Psi\Psi}(v_2, v_3)\pi_5(\boldsymbol{u}|\boldsymbol{v})}{s^{(1)}_{\Psi\Psi}(v_2, v_3)}\,, \tag{A.26}$$

$$\pi_2(\boldsymbol{u}|\boldsymbol{v}) = \frac{\pi_4(\boldsymbol{u}|v_2, v_1, v_3) - s^{(2)}_{\Psi\Psi}(v_1, v_2)\pi_4(\boldsymbol{u}|\boldsymbol{v})}{s^{(1)}_{\Psi\Psi}(v_1, v_2)}\,, \tag{A.27}$$

$$\pi_1(\boldsymbol{u}|\boldsymbol{v}) = \frac{\pi_3(\boldsymbol{u}|v_2, v_1, v_3) - s^{(2)}_{\Psi\Psi}(v_1, v_2)\pi_3(\boldsymbol{u}|\boldsymbol{v})}{s^{(1)}_{\Psi\Psi}(v_1, v_2)}\,. \tag{A.28}$$

A.3. Holes and (anti)fermions

We move on to the final two examples. To start with, let us present expressions for two holes $\boldsymbol{u} = (u_1, u_2)$ to four fermions $\boldsymbol{v} = (v_1, v_2, v_3, v_4)$ transitions. The seed for the recursion is

$$\pi_6(\boldsymbol{u}|\boldsymbol{v}) = \frac{(u_1|v_1)_{-1/2}(u_1|v_2)_{-1/2}(u_2|v_3)_{3/2}(u_2|v_4)_{3/2}}{(u_1|u_2)_{-1}(u_1|u_2)_2(v_1|v_2)_1(v_1|v_3)_1(v_1|v_4)_1(v_2|v_3)_1(v_2|v_4)_1(v_3|v_4)_1}\,, \tag{A.29}$$

with the rest being

$$\pi_5(\boldsymbol{u}|\boldsymbol{v}) = \frac{\pi_6(\boldsymbol{u}|v_1, v_3, v_2, v_4) - s^{(2)}_{\Psi\Psi}(v_2, v_3)\pi_6(\boldsymbol{u}|\boldsymbol{v})}{s^{(1)}_{\Psi\Psi}(v_2, v_3)}\,, \tag{A.30}$$

$$\pi_3(\boldsymbol{u}|\boldsymbol{v}) = \frac{\pi_5(\boldsymbol{u}|v_1, v_3, v_2, v_4) - s^{(2)}_{\Psi\Psi}(v_1, v_2)\pi_5(\boldsymbol{u}|\boldsymbol{v})}{s^{(1)}_{\Psi\Psi}(v_1, v_2)}\,, \tag{A.31}$$

$$\pi_4(\boldsymbol{u}|\boldsymbol{v}) = \frac{\pi_5(\boldsymbol{u}|v_1, v_2, v_4, v_3) - s^{(2)}_{\Psi\Psi}(v_3, v_4)\pi_5(\boldsymbol{u}|\boldsymbol{v})}{s^{(1)}_{\Psi\Psi}(v_3, v_4)}\,, \tag{A.32}$$

$$\pi_2(\boldsymbol{u}|\boldsymbol{v}) = \frac{\pi_4(\boldsymbol{u}|v_2, v_1, v_3, v_4) - s^{(2)}_{\Psi\Psi}(v_1, v_2)\pi_4(\boldsymbol{u}|\boldsymbol{v})}{s^{(1)}_{\Psi\Psi}(v_1, v_2)}\,, \tag{A.33}$$

$$\pi_1(\boldsymbol{u}|\boldsymbol{v}) = \frac{\pi_2(\boldsymbol{u}|v_1, v_3, v_2, v_4) - s^{(2)}_{\Psi\Psi}(v_2, v_3)\pi_2(\boldsymbol{u}|\boldsymbol{v})}{s^{(1)}_{\Psi\Psi}(v_2, v_3)}\,. \tag{A.34}$$

Now, we demonstrate the case of two fermions and a hole on the bottom along with four antifermions on the top. The twisted component is

$$\pi_{12}(\boldsymbol{u}, \boldsymbol{v}|\boldsymbol{w}) \tag{A.35}$$
$$= \frac{(u_1|w_1)_0(u_1|w_2)_0(u_1|w_3)_0(u_2|w_1)_0(u_2|w_2)_0(u_2|w_4)_1(v_1|w_3)_{3/2}(v_1|w_4)_{3/2}}{(u_1|u_2)_{-1}(u_1|v_1)_{-3/2}(u_2|v_1)_{-3/2}(w_1|w_2)_1(w_1|w_3)_1(w_1|w_4)_1(w_2|w_3)_1(w_2|w_4)_1(w_3|w_4)_1}\,,$$

with the remaining ones emerging from the Watson equations,

$$\pi_{11}(\boldsymbol{u}, \boldsymbol{v}|\boldsymbol{w}) = \frac{\pi_{12}(\boldsymbol{u}, \boldsymbol{v}|w_1, w_3, w_2, w_4) - s^{(2)}_{\Psi\Psi}(w_2, w_3)\pi_{12}(\boldsymbol{u}, \boldsymbol{v}|\boldsymbol{w})}{s^{(1)}_{\Psi\Psi}(w_2, w_3)}\,, \tag{A.36}$$

$$\pi_9(\boldsymbol{u}, \boldsymbol{v}|\boldsymbol{w}) = \frac{\pi_{12}(\boldsymbol{u}, \boldsymbol{v}|w_1, w_2, w_4, w_3) - s^{(2)}_{\Psi\Psi}(w_3, w_4)\pi_{12}(\boldsymbol{u}, \boldsymbol{v}|\boldsymbol{w})}{s^{(1)}_{\Psi\Psi}(w_3, w_4)}\,, \tag{A.37}$$

$$\pi_{10}(\boldsymbol{u}, \boldsymbol{v}|\boldsymbol{w}) = \frac{\pi_{11}(\boldsymbol{u}, \boldsymbol{v}|w_2, w_1, w_3, w_4) - s^{(2)}_{\Psi\Psi}(w_1, w_2)\pi_{11}(\boldsymbol{u}, \boldsymbol{v}|\boldsymbol{w})}{s^{(1)}_{\Psi\Psi}(w_1, w_2)}\,, \tag{A.38}$$

$$\pi_8(\boldsymbol{u},\boldsymbol{v}|\boldsymbol{w}) = \frac{\pi_{11}(\boldsymbol{u},\boldsymbol{v}|w_1,w_2,w_4,w_3) - s^{(2)}_{\Psi\Psi}(w_3,w_4)\pi_{11}(\boldsymbol{u},\boldsymbol{v}|\boldsymbol{w})}{s^{(1)}_{\Psi\Psi}(w_3,w_4)}\,, \tag{A.39}$$

$$\pi_7(\boldsymbol{u},\boldsymbol{v}|\boldsymbol{w}) = \frac{\pi_{10}(\boldsymbol{u},\boldsymbol{v}|w_1,w_2,w_4,w_3) - s^{(2)}_{\Psi\Psi}(w_3,w_4)\pi_{10}(\boldsymbol{u},\boldsymbol{v}|\boldsymbol{w})}{s^{(1)}_{\Psi\Psi}(w_3,w_4)}\,, \tag{A.40}$$

$$\pi_6(\boldsymbol{u},\boldsymbol{v}|\boldsymbol{w}) = \frac{\pi_9(\boldsymbol{u},\boldsymbol{v}|w_1,w_3,w_2,w_4) - s^{(2)}_{\Psi\Psi}(w_2,w_3)\pi_9(\boldsymbol{u},\boldsymbol{v}|\boldsymbol{w})}{s^{(1)}_{\Psi\Psi}(w_2,w_3)}\,, \tag{A.41}$$

$$\pi_5(\boldsymbol{u},\boldsymbol{v}|\boldsymbol{w}) = \frac{\pi_8(\boldsymbol{u},\boldsymbol{v}|w_1,w_3,w_2,w_4) - s^{(2)}_{\Psi\Psi}(w_2,w_3)\pi_8(\boldsymbol{u},\boldsymbol{v}|\boldsymbol{w})}{s^{(1)}_{\Psi\Psi}(w_2,w_3)}\,, \tag{A.42}$$

$$\pi_4(\boldsymbol{u},\boldsymbol{v}|\boldsymbol{w}) = \frac{\pi_7(\boldsymbol{u},\boldsymbol{v}|w_1,w_3,w_2,w_4) - s^{(2)}_{\Psi\Psi}(w_2,w_3)\pi_7(\boldsymbol{u},\boldsymbol{v}|\boldsymbol{w})}{s^{(1)}_{\Psi\Psi}(w_2,w_3)}\,, \tag{A.43}$$

$$\pi_3(\boldsymbol{u},\boldsymbol{v}|\boldsymbol{w}) = \frac{\pi_6(\boldsymbol{u},\boldsymbol{v}|w_2,w_1,w_3,w_4) - s^{(2)}_{\Psi\Psi}(w_1,w_2)\pi_6(\boldsymbol{u},\boldsymbol{v}|\boldsymbol{w})}{s^{(1)}_{\Psi\Psi}(w_1,w_2)}\,, \tag{A.44}$$

$$\pi_2(\boldsymbol{u},\boldsymbol{v}|\boldsymbol{w}) = \frac{\pi_5(\boldsymbol{u},\boldsymbol{v}|w_2,w_1,w_3,w_4) - s^{(2)}_{\Psi\Psi}(w_1,w_2)\pi_5(\boldsymbol{u},\boldsymbol{v}|\boldsymbol{w})}{s^{(1)}_{\Psi\Psi}(w_1,w_2)}\,, \tag{A.45}$$

$$\pi_1(\boldsymbol{u},\boldsymbol{v}|\boldsymbol{w}) = \frac{\pi_4(\boldsymbol{u},\boldsymbol{v}|w_2,w_1,w_3,w_4) - s^{(2)}_{\Psi\Psi}(w_1,w_2)\pi_4(\boldsymbol{u},\boldsymbol{v}|\boldsymbol{w})}{s^{(1)}_{\Psi\Psi}(w_1,w_2)}\,. \tag{A.46}$$

Appendix B. Supplementary material

Supplementary material related to this article can be found online at http://dx.doi.org/10.1016/j.nuclphysb.2017.08.011.

References

[1] L.F. Alday, D. Gaiotto, J. Maldacena, A. Sever, P. Vieira, An operator product expansion for polygonal null Wilson loops, J. High Energy Phys. 1104 (2011) 088, arXiv:1006.2788 [hep-th].
[2] B. Basso, A. Sever, P. Vieira, Spacetime and flux tube S-matrices at finite coupling for N = 4 supersymmetric Yang–Mills theory, Phys. Rev. Lett. 111 (2013) 091602, arXiv:1303.1396 [hep-th].
[3] A.V. Belitsky, A.S. Gorsky, G.P. Korchemsky, Logarithmic scaling in gauge/string correspondence, Nucl. Phys. B 748 (2006) 24, arXiv:hep-th/0601112.
[4] B. Basso, Exciting the GKP string at any coupling, Nucl. Phys. B 857 (2012) 254, arXiv:1010.5237 [hep-th].
[5] B. Basso, A. Sever, P. Vieira, Space-time S-matrix and flux tube S-matrix, II: extracting and matching data, J. High Energy Phys. 1401 (2014) 008, arXiv:1306.2058 [hep-th].
[6] B. Basso, A. Sever, P. Vieira, Space-time S-matrix and flux-tube S-matrix, III: the two-particle contributions, J. High Energy Phys. 1408 (2014) 085, arXiv:1402.3307 [hep-th].
[7] A.V. Belitsky, Nonsinglet pentagons and NHMV amplitudes, Nucl. Phys. B 896 (2015) 493, arXiv:1407.2853 [hep-th].
[8] B. Basso, A. Sever, P. Vieira, Space-time S-matrix and flux-tube S-matrix, IV: gluons and fusion, J. High Energy Phys. 1409 (2014) 149, arXiv:1407.1736 [hep-th].
[9] A.V. Belitsky, Fermionic pentagons and NMHV hexagon, Nucl. Phys. B 894 (2015) 108, arXiv:1410.2534 [hep-th].
[10] A.V. Belitsky, On factorization of multiparticle pentagons, Nucl. Phys. B 897 (2015) 346, arXiv:1501.06860 [hep-th].
[11] B. Basso, J. Caetano, L. Cordova, A. Sever, P. Vieira, OPE for all helicity amplitudes, J. High Energy Phys. 1508 (2015) 018, arXiv:1412.1132 [hep-th].

[12] B. Basso, J. Caetano, L. Cordova, A. Sever, P. Vieira, OPE for all helicity amplitudes, II: form factors and data analysis, arXiv:1508.02987 [hep-th].
[13] A.V. Belitsky, S.E. Derkachov, A.N. Manashov, Quantum mechanics of null polygonal Wilson loops, Nucl. Phys. B 882 (2014) 303, arXiv:1401.7307 [hep-th].
[14] A.V. Belitsky, Supersymmetric quantum mechanics of the flux tube, Nucl. Phys. B 913 (2016) 551, arXiv:1604.00418 [hep-th].
[15] B. Basso, A. Sever, P. Vieira, Collinear limit of scattering amplitudes at strong coupling, Phys. Rev. Lett. 113 (2014) 261604, arXiv:1405.6350 [hep-th].
[16] B. Basso, A. Sever, P. Vieira, Hexagonal Wilson loops in planar $\mathcal{N} = 4$ SYM theory at finite coupling, J. Phys. A 49 (2016) 41LT01, arXiv:1508.03045 [hep-th].
[17] B. Basso, A.V. Belitsky, Luescher formula for GKP string, Nucl. Phys. B 860 (2012) 1, arXiv:1108.0999 [hep-th].
[18] B. Basso, A. Rej, Bethe Ansätze for GKP strings, Nucl. Phys. B 879 (2014) 162, arXiv:1306.1741 [hep-th].
[19] A.B. Zamolodchikov, A.B. Zamolodchikov, Relativistic factorized S matrix in two-dimensions having O(N) isotopic symmetry, Nucl. Phys. B 133 (1978) 525.
[20] B. Berg, M. Karowski, P. Weisz, V. Kurak, Factorized U(N) symmetric S-matrices in two-dimensions, Nucl. Phys. B 134 (1978) 125.
[21] L.F. Alday, J.M. Maldacena, Comments on operators with large spin, J. High Energy Phys. 0711 (2007) 019, arXiv:0708.0672 [hep-th].
[22] A.V. Belitsky, Nonperturbative enhancement of superloop at strong coupling, Nucl. Phys. B 911 (2016) 425, arXiv:1512.00555 [hep-th].
[23] A. Bonini, D. Fioravanti, S. Piscaglia, M. Rossi, On the contribution of scalars to $\mathcal{N} = 4$ SYM amplitudes, Phys. Rev. D 95 (2017) 041902, arXiv:1607.02084 [hep-th].